

RIGOROUS NETWORK ADJUSTMENT OF GPS CARRIER PHASES FOR AIRBORNE POSITIONING VIA TROPOSPHERIC ERROR VARIANCE-COVARIANCE MODELLING

R. Radovanovic, N. El-Sheimy, W.F. Teskey
Department of Geomatics Engineering
University of Calgary, Canada
Tel : +1 (403) 220-8785
Fax : +1 (403) 284-1980
Email : rsradova@ucalgary.ca

KEYWORDS : Network Adjustment, Variance-Covariance Modelling, Kinematic Positioning, Tropospheric Modelling

1.0 ABSTRACT

A method of rigorously combining data collected at several ground stations and a mobile platform is presented, based on the use of an overconstrained network adjustment, with the coordinates of the ground stations held as fixed. As well, a model of the variance-covariance matrix of observations is developed for use on medium length baselines (10 – 500 kilometres) where the effect of residual tropospheric errors dominate. A scheme is presented which allows parameters of the model to be derived from the carrier phase data collected in a static reference network.

The importance of proper modelling of the variance-covariance matrix is illustrated using a network of six reference receivers and a static receiver to be positioned. Typically, the epoch-to-epoch positioning of the remote receiver would be derived by processing six reference-to-remote baselines, and then combining the individual results using a weighted mean-scheme. It is shown that the difference in the resulting position solution using this method can vary by up to ten centimetres in height from that obtained by the rigorous network method. However, it is shown that incorrectly modelling the variance-covariance matrix can also bias the results. If the variance-covariance matrix is correctly modelled, positioning accuracies of two centimetres are possible using baselines ranging in length from 20 kilometres to 400 kilometres. As well, the statistic estimates returned from the adjustment are consistent with the variation in the epoch-to-epoch positioning estimates.

2.0 INTRODUCTION

Traditional techniques of using GPS for airborne positioning have relied on the use of an onboard receiver and a single ground base station. If data from multiple ground stations is available, the usual procedure is to process each ground to air baseline separately and combine the final position estimates, often using a weighted mean scheme based the accuracy estimates for each baseline. Although a simple procedure, it assumes that the baselines processed are independent, which is not true, even from mathematical considerations. This paper presents a method of rigorously combining data collected at several ground stations and a mobile platform in a overconstrained network adjustment, with the coordinates of the ground stations held as fixed.

The concept of double differencing carrier phases is well known and widely practised. Since carrier phases collected at two receivers are affected by similar errors, differencing significantly cancels out these correlated errors. This often allows the integer carrier ambiguities to be fixed. However, it is interesting that despite the implicit acknowledgement that carrier phases are correlated, the original physical correlations between phases are usually neglected in the diagonal variance-covariance (CI) matrix of observations often used. Even if mathematical correlations of the double-differences are modelled correctly (Hofmann-Wellenhof et al, 1997), the resulting statistics are still in error due to the misleading CI matrix originally assumed. The position estimates can also be biased, due to incorrect weighting of the double differences created. One aspect of the adjustment method presented herein is the use of a fully populated CI matrix, created by a model of tropospheric covariances derived from data collected at the ground stations.

3.0 CORRELATION OF GPS CARRIER PHASES

Consider the situation of three receivers making simultaneous measurements to three satellites as shown in Figure (1). The covariance of any two measurements between receivers A and B and satellites i and j is expressed as

$$\begin{aligned} \sigma_{ij}^{AB} &= E\left[\left(\phi_i^A - E(\phi_i^A)\right) \cdot \left(\phi_j^B - E(\phi_j^B)\right)\right] \\ &= E\left[\left(\frac{1}{\lambda} \left[c \cdot (\delta t_{sati}^A - \delta t_{recA}^i) + \delta r_i^A + \delta T_i^A - \delta I_i^A + m_i^A + n_i^A \right] \right) \cdot \right. \\ &\quad \left. \left(\frac{1}{\lambda} \left[c \cdot (\delta t_{satj}^B - \delta t_{recB}^j) + \delta r_j^B + \delta T_j^B - \delta I_j^B + m_j^B + n_j^B \right] \right) \right] \end{aligned} \quad (1)$$

where

Φ	...	measured fractional phase (cycles)
λ	...	carrier wavelength (m)
c	...	speed of light (m/s)
$\delta t_{sat} / \delta t_{rec}$...	satellite clock / receiver clock offset (s)
δr	...	orbital error projected along line-of-sight (m)
T	...	tropospheric delay (m)
I	...	ionospheric delay (m)

- m_ϕ ... multipath on carrier (m)
- n_ϕ ... noise on carrier (m)

Note that the expected value of ϕ_i^A is equal to the range and ambiguity of the carrier phases and that the error sources are assumed to have zero mean.

Equation (1) can be further simplified by assuming that the error sources are physically uncorrelated among themselves. This is valid since each error source stems from a different physical process. For example, there is no reason why the value of the satellite clock offset should at all affect the actual tropospheric delay constrained within a measured carrier phase. As a result, the variance expression becomes :

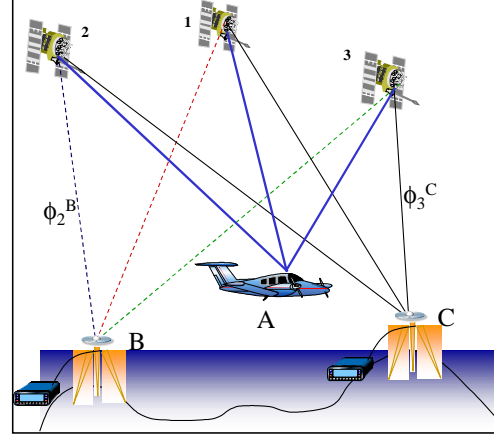


Figure 1. Example of GPS Observation Set

$$\begin{aligned} \sigma_{ij}^{AB} &= \frac{1}{\lambda^2} E \left[c \cdot (\delta t_{sati}^A \delta t_{satj}^B + \delta t_{recA}^i \delta t_{recB}^j) + \delta r_i^A \delta r_j^B + \delta T_i^A \delta T_j^B - \delta I_i^A \delta I_j^B + m_i^A m_j^B + n_i^A n_j^B \right] \\ &= \sigma_{ij}^{AB} (\delta t_{sat}) + \sigma_{ij}^{AB} (\delta t_{rec}) + \sigma_{ij}^{AB} (\delta r) + \sigma_{ij}^{AB} (\delta T) + \sigma_{ij}^{AB} (\delta I) + \sigma_{ij}^{AB} (m) + \sigma_{ij}^{AB} (n) \end{aligned} \quad (2)$$

where the covariances of the individual error sources have been introduced. Note that the tropospheric and ionospheric terms are *residual* errors, or errors remaining after a model has been applied.

For the nine observations indicated in Figure (1), the variance-covariance matrix for the set can be written as :

$$Cl = \begin{bmatrix} \sigma_1^{A^2} & \sigma_{12}^A & \sigma_{13}^A & \sigma_1^{AB} & \sigma_{12}^{AB} & \sigma_{13}^{AB} & \sigma_1^{AC} & \sigma_{12}^{AC} & \sigma_{13}^{AC} \\ \sigma_{21}^A & \sigma_2^{A^2} & \sigma_{23}^A & \sigma_{21}^{AB} & \sigma_2^{AB} & \sigma_{23}^{AB} & \sigma_{21}^{AC} & \sigma_2^{AC} & \sigma_{23}^{AC} \\ \sigma_{31}^A & \sigma_{32}^A & \sigma_3^{A^2} & \sigma_{31}^{AB} & \sigma_{32}^{AB} & \sigma_3^{AB} & \sigma_{31}^{AC} & \sigma_{32}^{AC} & \sigma_3^{AC} \\ \sigma_1^{BA} & \sigma_{12}^{BA} & \sigma_{13}^{BA} & \sigma_1^{B^2} & \sigma_{12}^B & \sigma_{13}^B & \sigma_1^{BC} & \sigma_{12}^{BC} & \sigma_{13}^{BC} \\ \sigma_{21}^{BA} & \sigma_2^{BA} & \sigma_{23}^{BA} & \sigma_{21}^B & \sigma_2^{B^2} & \sigma_{23}^B & \sigma_{21}^{BC} & \sigma_2^{BC} & \sigma_{23}^{BC} \\ \sigma_{31}^{BA} & \sigma_{32}^{BA} & \sigma_3^{BA} & \sigma_{31}^B & \sigma_{32}^B & \sigma_3^{B^2} & \sigma_{31}^{BC} & \sigma_{32}^{BC} & \sigma_3^{BC} \\ \sigma_1^{CA} & \sigma_{12}^{CA} & \sigma_{13}^{CA} & \sigma_1^{CB} & \sigma_{12}^{CB} & \sigma_{13}^{CB} & \sigma_1^{C^2} & \sigma_{12}^C & \sigma_{13}^C \\ \sigma_{21}^{CA} & \sigma_2^{CA} & \sigma_{23}^{CA} & \sigma_{21}^{CB} & \sigma_2^{CB} & \sigma_{23}^{CB} & \sigma_{21}^C & \sigma_2^{C^2} & \sigma_{23}^C \\ \sigma_{31}^{CA} & \sigma_{32}^{CA} & \sigma_3^{CA} & \sigma_{31}^{CB} & \sigma_{32}^{CB} & \sigma_3^{CB} & \sigma_{31}^C & \sigma_{32}^C & \sigma_3^{C^2} \end{bmatrix} \quad (3)$$

Only four basic forms of variances exist, namely σ_i^A , σ_i^{AB} , σ_{ij}^A , σ_{ij}^{AB} . Furthermore, elements of the form σ_{ij}^A are equal to their corresponding elements of the form σ_{ji}^A . As well, elements of the form σ_i^{AB} are equal to elements of the form σ_i^{BA} . This also holds for

pairs of elements with the form σ_{ij}^{AB} and σ_{ji}^{BA} , respectively. However, elements σ_{ij}^{AB} are *not* necessarily equal to elements σ_{ji}^{AB} or σ_{ij}^{BA} . Applying these equalities, it can be shown that the above matrix is symmetric, as expected.

3.1 Double Differenced Covariances

One consequence of forming double differences is that, given a set of double differences, the non-redundant differences are *correlated*. The nature of the correlation can be determined via propagation of variances. For the set of observations presented in section 2.1, the resulting covariance matrix of one non-redundant differencing scheme is :

$$Cl^{DD} = BCIB^T = \begin{bmatrix} 1 & -1 & 0 & -1 & 1 & 0 & 0 & 0 & 0 \\ 1 & 0 & -1 & -1 & 0 & 1 & 0 & 0 & 0 \\ 1 & -1 & 0 & 0 & 0 & 0 & -1 & 1 & 0 \\ 1 & 0 & -1 & 0 & 0 & 0 & -1 & 0 & 1 \end{bmatrix} \cdot Cl \cdot \begin{bmatrix} 1 & 1 & 1 & 1 \\ -1 & 0 & -1 & 0 \\ 0 & -1 & 0 & -1 \\ -1 & -1 & 0 & 0 \\ 1 & 0 & 0 & 0 \\ 0 & 1 & 0 & 0 \\ 0 & 0 & -1 & -1 \\ 0 & 0 & 1 & 0 \\ 0 & 0 & 0 & -1 \end{bmatrix} \quad (4)$$

$$= \begin{bmatrix} \sigma^2(\nabla\Delta_{12}^{AB}) & \sigma(\nabla\Delta_{12}^{AB}, \nabla\Delta_{13}^{AB}) & \sigma(\nabla\Delta_{12}^{AB}, \nabla\Delta_{12}^{AC}) & \sigma(\nabla\Delta_{12}^{AB}, \nabla\Delta_{13}^{AC}) \\ \sigma(\nabla\Delta_{12}^{AB}, \nabla\Delta_{13}^{AB}) & \sigma^2(\nabla\Delta_{13}^{AB}) & \sigma(\nabla\Delta_{13}^{AB}, \nabla\Delta_{12}^{AC}) & \sigma(\nabla\Delta_{13}^{AB}, \nabla\Delta_{13}^{AC}) \\ \sigma(\nabla\Delta_{12}^{AB}, \nabla\Delta_{12}^{AC}) & \sigma(\nabla\Delta_{13}^{AB}, \nabla\Delta_{12}^{AC}) & \sigma^2(\nabla\Delta_{12}^{AC}) & \sigma(\nabla\Delta_{12}^{AC}, \nabla\Delta_{13}^{AC}) \\ \sigma(\nabla\Delta_{12}^{AB}, \nabla\Delta_{13}^{AC}) & \sigma(\nabla\Delta_{13}^{AB}, \nabla\Delta_{13}^{AC}) & \sigma(\nabla\Delta_{12}^{AC}, \nabla\Delta_{13}^{AC}) & \sigma^2(\nabla\Delta_{13}^{AC}) \end{bmatrix}$$

where Cl is given by equation (3).

The variance-covariance matrix shown in equation (4) is fully-populated and symmetric. The explicit form of each element can be derived by completing the multiplication indicated in equation (4), given the Cl matrix shown in equation (3). The results are as follows :

$$\begin{aligned}
\sigma^2(\nabla\Delta_{12}^{AB}) &= \sigma_1^{A^2} + \sigma_1^{B^2} + \sigma_2^{A^2} + \sigma_2^{B^2} - 2\sigma_{12}^A - 2\sigma_{12}^B - 2\sigma_1^{AB} - 2\sigma_2^{AB} + 2\sigma_{12}^{AB} + 2\sigma_{21}^{AB} \\
\sigma^2(\nabla\Delta_{12}^{AB}, \nabla\Delta_{13}^{AB}) &= \sigma_1^{A^2} + \sigma_1^{B^2} - \sigma_{12}^A - \sigma_{13}^A - \sigma_{12}^B - \sigma_{13}^B + \sigma_{23}^A + \sigma_{23}^B - 2\sigma_1^{AB} + \sigma_{12}^{AB} + \sigma_{21}^{AB} \\
&\quad + \sigma_{13}^{AB} + \sigma_{31}^{AB} - \sigma_{32}^{AB} - \sigma_{23}^{AB} \\
\sigma^2(\nabla\Delta_{12}^{AB}, \nabla\Delta_{12}^{AC}) &= \sigma_1^{A^2} + \sigma_2^{A^2} - \sigma_1^{AB} - \sigma_2^{AB} - \sigma_1^{AC} - \sigma_2^{AC} - 2\sigma_{12}^A + \sigma_{12}^{AB} + \sigma_{21}^{AB} + \sigma_{12}^{AC} + \sigma_{21}^{AC} \\
&\quad + \sigma_1^{BC} + \sigma_2^{BC} - \sigma_{12}^{BC} - \sigma_{21}^{BC} \\
\sigma^2(\nabla\Delta_{12}^{AB}, \nabla\Delta_{13}^{AC}) &= \sigma_1^{A^2} - \sigma_{12}^A - \sigma_{13}^A - \sigma_1^{AB} + \sigma_1^{BC} - \sigma_1^{AC} + \sigma_{23}^A + \sigma_{12}^{AB} + \sigma_{31}^{AB} - \sigma_{32}^{AB} \\
&\quad + \sigma_{21}^{AC} - \sigma_{21}^{BC} + \sigma_{13}^{AC} - \sigma_{23}^{AC} - \sigma_{13}^{BC} + \sigma_{23}^{BC}
\end{aligned} \tag{5}$$

where the elements :

- $\sigma(\nabla\Delta_{12}^{AB}, \nabla\Delta_{12}^{AB})$, $\sigma(\nabla\Delta_{13}^{AB}, \nabla\Delta_{13}^{AB})$, $\sigma(\nabla\Delta_{12}^{AC}, \nabla\Delta_{12}^{AC})$, and $\sigma(\nabla\Delta_{13}^{AC}, \nabla\Delta_{13}^{AC})$
- $\sigma^2(\nabla\Delta_{12}^{AB}, \nabla\Delta_{13}^{AB})$ and $\sigma^2(\nabla\Delta_{12}^{AC}, \nabla\Delta_{13}^{AC})$
- $\sigma^2(\nabla\Delta_{12}^{AB}, \nabla\Delta_{13}^{AC})$ and $\sigma^2(\nabla\Delta_{13}^{AB}, \nabla\Delta_{12}^{AC})$
- $\sigma^2(\nabla\Delta_{13}^{AB}, \nabla\Delta_{13}^{AC})$ and $\sigma^2(\nabla\Delta_{12}^{AB}, \nabla\Delta_{12}^{AC})$

have similar forms, respectively.

Using the property of independence between physical processes described by equation (2), the variances described in equation (5) can be described as the sum of variances and covariances of each error source. For example,

$$\begin{aligned}
\sigma^2(\nabla\Delta_{12}^{AB}) &= \sigma^2(\nabla\Delta_{12}^{AB} t_{sat}) + \sigma^2(\nabla\Delta_{12}^{AB} t_{rec}) + \sigma^2(\nabla\Delta_{12}^{AB} n) + \sigma^2(\nabla\Delta_{12}^{AB} T) \\
&\quad + \sigma^2(\nabla\Delta_{12}^{AB} I) + \sigma^2(\nabla\Delta_{12}^{AB} m) + \sigma^2(\nabla\Delta_{12}^{AB} \delta r)
\end{aligned} \tag{6}$$

where each component has the same form as the total variance described in equation (5). This formulation is useful since it means that each error source can be independently analysed and the full double difference covariance matrix formed from individual error models. For example, Radovanovic et al, 2000 presents models for the multipath and noise error covariances and shows that the double differenced satellite and receiver clock error covariances are all zero. This paper focuses on developing models for the residual tropospheric error.

3.2 Tropospheric Error Covariance Model

Most modern tropospheric models combine a model of the zenith tropospheric delay and a mapping function to relate the zenith delay to that at lower elevations. In the case of double differenced observations, this model can be expressed as :

$$\Delta T_{12}^{AB} = (m(\epsilon_1^A) - m(\epsilon_2^A))I_Z^A - (m(\epsilon_1^B) - m(\epsilon_2^B))I_Z^B \tag{7}$$

where

$m(\varepsilon^A_1), m(\varepsilon^A_2) \dots$ mapping functions at station A to satellite 1 and satellite 2, respectively
 $T^A_z, T^B_z \dots$ zenith delays at stations A and B, respectively

Often the hydrostatic and wet components of the tropospheric delay are modeled separately, with each component preserving the form of equation (7). Models of the above form assume that the atmosphere has a certain refractivity profile with regard to altitude, and that it is homogenous from point-to-point. The real atmosphere of course is much more complex and as a result, a residual tropospheric delay error remains. This error is basically an integration of the point-to-point refractivity errors along the line-of-sight to the satellite. Assuming that the *variations* of refractivity are constant throughout the atmosphere, the delay error variance is then proportional to the path length of the observation ray. The path length is in turn proportional to the mapping function for the observation and so the delay variance can be written as :

$$\sigma_1^{A^2} = E(\delta T_1^A \cdot \delta T_1^A) = E(m(\varepsilon_1) \delta T_z^A \cdot m(\varepsilon_1) \delta T_z^A) = m(\varepsilon_1)^2 \sigma_T^2 \quad (8)$$

where

$\sigma_1^{A^2} \dots$ tropospheric error variance of observation to satellite 1
 $\sigma_T^2 \dots$ zenith tropospheric error variance

In the case of observations made from a station to two satellites, the residual tropospheric errors are expected to be correlated if the line-of-sights to the two satellites pass through the same region of atmosphere. From spherical trigonometry, the angle of separation between two observation line-of-sights, θ , can be written as :

$$\cos \theta = \sin \varepsilon_1 \sin \varepsilon_2 + \cos \varepsilon_1 \cos \varepsilon_2 \cos(A_1 - A_2) \quad (9)$$

where

$A_1, A_2 \dots$ azimuths of line-of-sights to satellites 1 and 2
 $\varepsilon_1, \varepsilon_2 \dots$ elevation angles to satellites 1 and 2

For satellites in the same region of the sky (θ near zero), the line-of-sight vectors pass through similar portions of the troposphere and as a result the respective delay errors are the sum of the integration of similar point-to-point refractivity errors. Thus the covariance of the two delay errors should be nearly equal to the variance of a single observation (or the covariance of an error with itself). For satellites in very different parts of the sky (θ near 180°), the point-to-point refractivity errors will be very uncorrelated and the covariance of the delays nearly equal to zero. As a result, the covariance of the delay errors will be modeled in similar fashion as the variance of a single delay, with an exponential factor added to take into account decorrelation with increasing angular separation.

$$\sigma_{12}^A = E(\delta T_1^A \cdot \delta T_2^A) = E(m(\varepsilon_1) \delta T_{z1}^A \cdot m(\varepsilon_2) \delta T_{z2}^A) = m(\varepsilon_1) m(\varepsilon_2) \exp(-\theta / \Omega) \cdot \sigma_T^2 \quad (10)$$

where

Ω ... experimentally determined correlation angle

A similar model is used for the correlation between observations made to the same satellite from different receivers. In this case, the tropospheric delay errors should cancel exactly if the receivers are collocated, and become completely uncorrelated if the receivers are separated by a great distance. Using an exponential decay model, the covariance is expressed as :

$$\sigma_1^{AB} = E(\delta T_1^A \cdot \delta T_1^B) = E(m(\varepsilon_1^A) \delta T_{Z1}^A \cdot m(\varepsilon_1^B) \delta T_{Z1}^B) = m(\varepsilon_1)^2 \exp(-d/D) \cdot \sigma_T^2 \quad (11)$$

where

d ... separation distance between receivers

D ... correlation distance

and the mapping functions to the satellite are assumed to be equal since the elevation angles at each receiver are nearly equal (roughly 0.3° difference for a 100km separation).

The final covariance to model is that of observations made to different satellites from different receivers. The result is a composite of equations (10) and (11), yielding :

$$\sigma_{12}^{AB} = E(\delta T_1^A \cdot \delta T_2^B) = E(m(\varepsilon_1^A) \delta T_{Z1}^A \cdot m(\varepsilon_2^B) \delta T_{Z2}^B) = m(\varepsilon_1) m(\varepsilon_2) \exp(-\theta/\Omega) \exp(-d/D) \cdot \sigma_T^2 \quad (12)$$

By using the models for the tropospheric error variances and covariances and substituting them into equation (5), the double differenced tropospheric error covariances can be derived. After collecting like terms, the resulting expressions are :

$$\begin{aligned} \sigma^2(\nabla \Delta_{12}^{AB}) &= 2 \cdot \left(m(\varepsilon_1)^2 + m(\varepsilon_2)^2 - 2m(\varepsilon_1)m(\varepsilon_2) \exp(-\theta_{12}/\Omega) \right) \cdot \sigma_T^2 (1 - \exp(-d_{AB}/D)) \\ \sigma^2(\nabla \Delta_{12}^{AB}, \nabla \Delta_{13}^{AB}) &= 2 \cdot \left(\begin{aligned} &m(\varepsilon_1)^2 + m(\varepsilon_2)m(\varepsilon_1) \exp(-\theta_{23}/\Omega) - m(\varepsilon_1)m(\varepsilon_2) \exp(-\theta_{12}/\Omega) \\ &- m(\varepsilon_1)m(\varepsilon_3) \exp(-\theta_{13}/\Omega) \end{aligned} \right) \\ &\quad \cdot \sigma_T^2 (1 - \exp(-d_{AB}/D)) \\ \sigma^2(\nabla \Delta_{12}^{AB}, \nabla \Delta_{12}^{AC}) &= \left(m(\varepsilon_1)^2 + m(\varepsilon_2)^2 - 2m(\varepsilon_1)m(\varepsilon_2) \exp(-\theta_{12}/\Omega) \right) \\ &\quad \cdot \sigma_T^2 (1 + \exp(-d_{BC}/D) - \exp(-d_{AB}/D) - \exp(-d_{AC}/D)) \\ \sigma^2(\nabla \Delta_{12}^{AB}, \nabla \Delta_{13}^{AC}) &= \left(\begin{aligned} &m(\varepsilon_1)^2 + m(\varepsilon_2)m(\varepsilon_1) \exp(-\theta_{23}/\Omega) - m(\varepsilon_1)m(\varepsilon_2) \exp(-\theta_{12}/\Omega) \\ &- m(\varepsilon_1)m(\varepsilon_3) \exp(-\theta_{13}/\Omega) \end{aligned} \right) \\ &\quad \cdot \sigma_T^2 (1 + \exp(-d_{BC}/D) - \exp(-d_{AB}/D) - \exp(-d_{AC}/D)) \end{aligned} \quad (13)$$

Note that the variances all decrease towards zero as receiver separation goes to zero and the satellite line-of-sights become coincident. This is expected since the tropospheric errors become increasingly correlated and thus cancel out. At the other extreme, the double differenced variance simply becomes twice the accuracy of the tropospheric model itself, as no cancellation occurs.

From equation (13), it is apparent that only three unknowns are required to completely model the double differenced tropospheric error variances and covariances : Ω , D and σ_T^2 . These can all be derived from data collected at a network of reference receivers. It is expected that these parameters will vary with time, as they are functions of the tropospheric model accuracy and the variability of the real atmosphere.

4.0 DETERMINATION OF TROPOSPHERIC COVARIANCE FROM NETWORK DATA

To determine the feasibility of modeling the residual tropospheric covariance as described above, a network of nine reference stations forming part of the Southern California Integrated GPS Network was used. The network configuration is shown in Figure (2). Station elevations ranged from -83 to 1567 meters above the WGS84 ellipsoid and receiver separations varied from 30 to 464 kilometres. Data was collected at 30 second intervals using ASHTECH Z-XII3 receivers and reference coordinates were generated by processing a full day of dual-frequency data using the GrafNetTM static baseline processing software.

Dual frequency data collected was used to form the ionospheric-free observable (IF), via the phase combination :

$$\phi_{IF} = \phi_{L1} - \frac{f_2}{f_1} \phi_{L2} \quad (14)$$

where

$\phi_{L1}, \phi_{L2} \dots$ phases measured on L1 and L2
 $f_1, f_2 \dots$ L1 and L2 frequencies (1575.24 MHz and 1227.60 MHz, respectively).

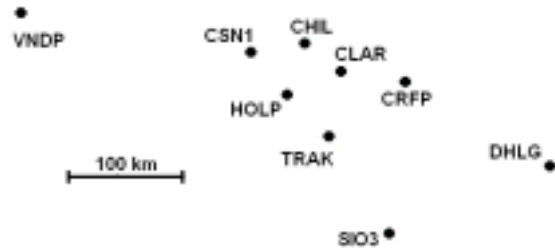


Figure 2. Reference Network Map

Although the ambiguity on the IF observable is not integer, it is a linear combination of L1 and L2 ambiguities, namely :

$$N_{IF} = N_{L1} - \frac{f_2}{f_1} N_{L2} \quad (15)$$

where the ambiguities N_{L1}, N_{L2} are determined using the float IF ambiguity, the resolved widelane ambiguity, and the relationship (Raquet, 1998) :

$$N_{L1} = \text{round} \left(\frac{N_{IF}^{FLOAT} - (f_2 / f_1) N_{WL}}{1 - f_2 / f_1} \right) \quad (16)$$

where

N_{IF}^{FLOAT}	...	float IF ambiguity
N_{WL}	...	fixed widelane ambiguity

This results in a highly accurate observable that is free of first-order ionospheric effects and thus desirable for isolating tropospheric effects.

Using data from the nine reference stations, double differences for 36 reference-station pairs were calculated using a 16 hours of data with 30 second data sampling, yielding approximately 500 000 double differences. The known coordinates of the reference stations were used to compute theoretic ranges to the satellites and remove them from the double differences. As well, the ambiguities were resolved and removed, leaving double differenced noise, multipath, tropospheric and orbital effects. Due to the limited extent of the network, broadcast orbits were used. Furthermore, the UNB3 tropospheric model (Collins, 1999) was applied since it does not require surface meteorological parameters, which the authors felt increased its applicability to airborne positioning.

The double differenced samples were then grouped according to the elevation angle of the low satellite into 2° bins and the root-mean-square (RMS) and mean of each bin was calculated. At all times the elevation of the base satellite remained above 50° . The results for all baselines are shown in Figures (3) and (4). The mean error is significant, especially for low elevation satellites.

Figure (5) shows the mean values plotted against receiver height separation. The figure reveals a linear trend in the mean errors. As a result, the authors decided to augment the UNB3 model with a simple relative delay model composed of an overall zenith bias and a relative bias linearly dependant on receiver height separation. The model was formed as :

$$\Delta\delta T_1^{AB} = (m(\epsilon_1^A) - m(\epsilon_0^A)) \cdot \Delta\delta T^{AB} - (m(\epsilon_1^B) - m(\epsilon_0^B) - m(\epsilon_1^A) + m(\epsilon_0^A)) \cdot \Delta\delta T \quad (17)$$

where

$\Delta\delta T_1^{AB}$...	differential tropospheric correction
$\Delta\delta T^{AB}$...	relative bias with $\Delta\delta T^{AB} = c \cdot (H_A - H_B)$
$\Delta\delta T$...	overall tropospheric model bias
$m(\epsilon_1^A), m(\epsilon_0^A)$...	mapping function at receiver A to satellite 1 and the base satellite, respectively

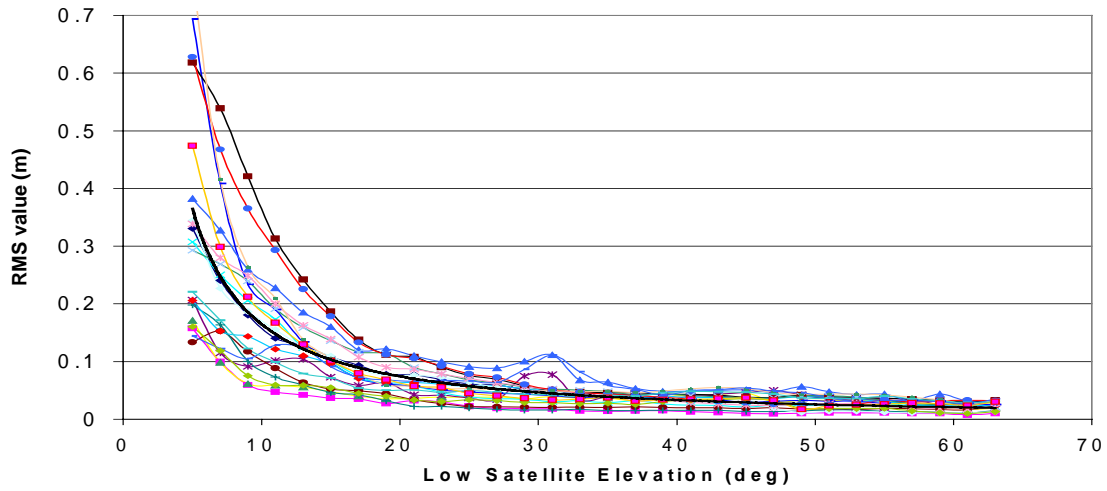


Figure 3. RMS Scatter of Double Differenced Samples.

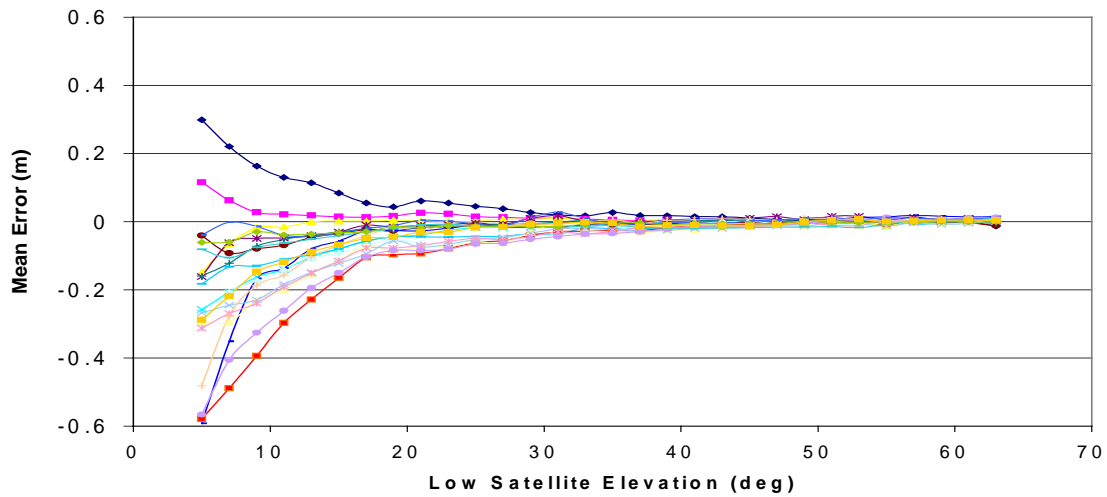


Figure 4. Mean Error of Double Differences

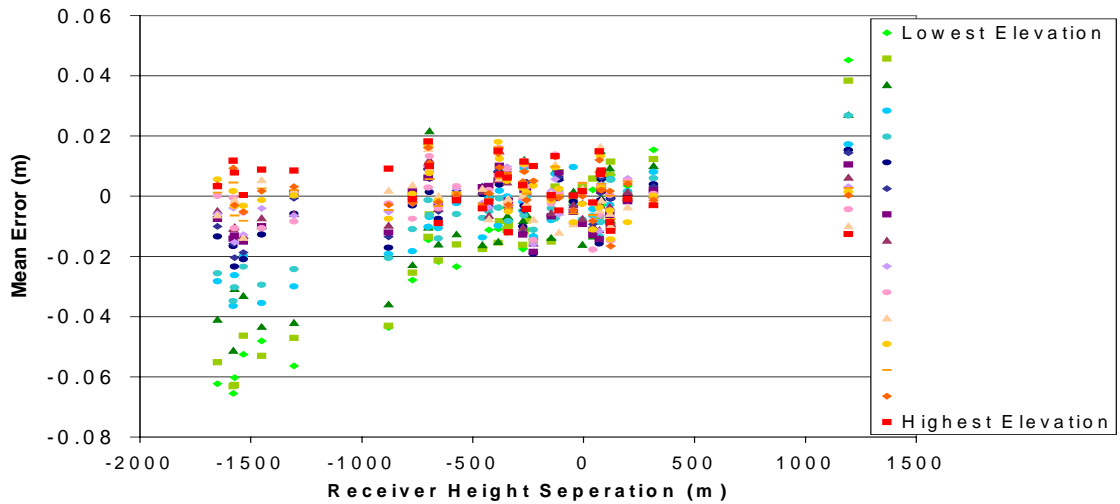


Figure 5. Mean Error of Double Differences versus Receiver Height Separation.

A least-squares adjustment was performed using the mean values to determine the values of c and $\Delta\delta T$. These were calculated to be $4.25e-5$ m/m and 0.12 m, respectively. Due to the small extent of the network and the corresponding small elevation angle differences between receivers to a common satellite, the value of the overall bias may be significantly in error. Figure (6) shows the RMS values of each elevation bin once the relative model has been applied. The figure shows significant improvement is, with the RMS values for elevations as low as 10° at the 10 centimetre level. As well, the mean errors become near zero for all elevation angles above 10° .

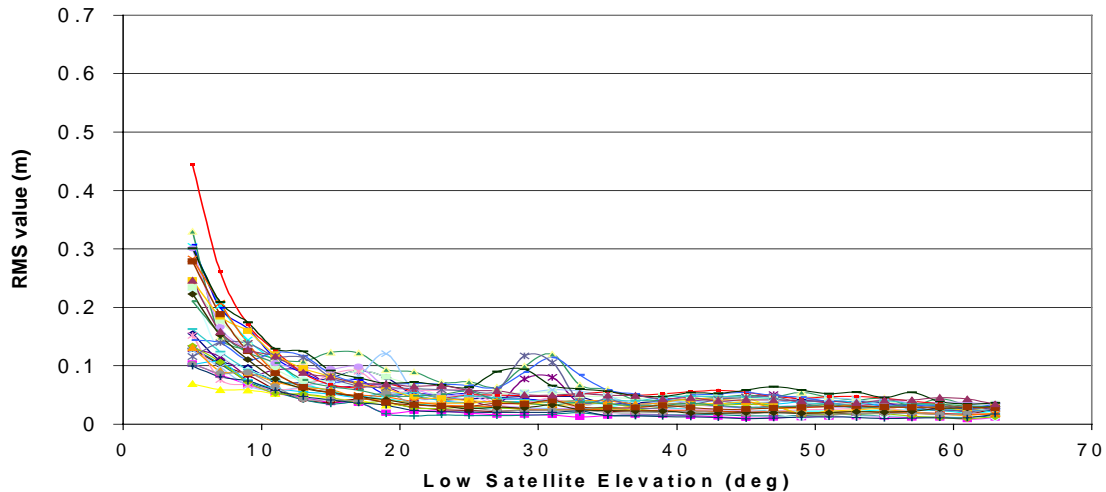


Figure 6. RMS Scatter of Double Differences After Applying Differential Tropo Model

According to the tropospheric covariance model presented in equation (13), the variance of the double differences at zenith should simply be the variance of the double differences at lower elevations divided by a polynomial composed of low and base satellite mapping functions. Figure (6) indicates that such a relationship holds.

To determine the correlation angle, Ω , values of Ω ranging from 0 (no correlation between satellite errors mapped to zenith) to infinity (full correlation) were used to map the variances of each elevation bin to zenith. The value of Ω which minimized the variations in the mapped zenith variances was considered the optimal one. Figure (7) shows a plot of the zenith variance variations for values of Ω and reveals that the correlation angle is near 20° .

It is important to note that the value of Ω depends on the quality of the tropospheric model. For example, if the model seriously mispredicts the zenith tropospheric delay, then all corrected satellites will have an error in their respective tropospheric corrections approximately equal to the mapping function multiplied by the zenith prediction error. This will make Ω very large. Conversely, if the model is very good, then remaining modeling errors will be very random and the correlation angle correspondingly small.

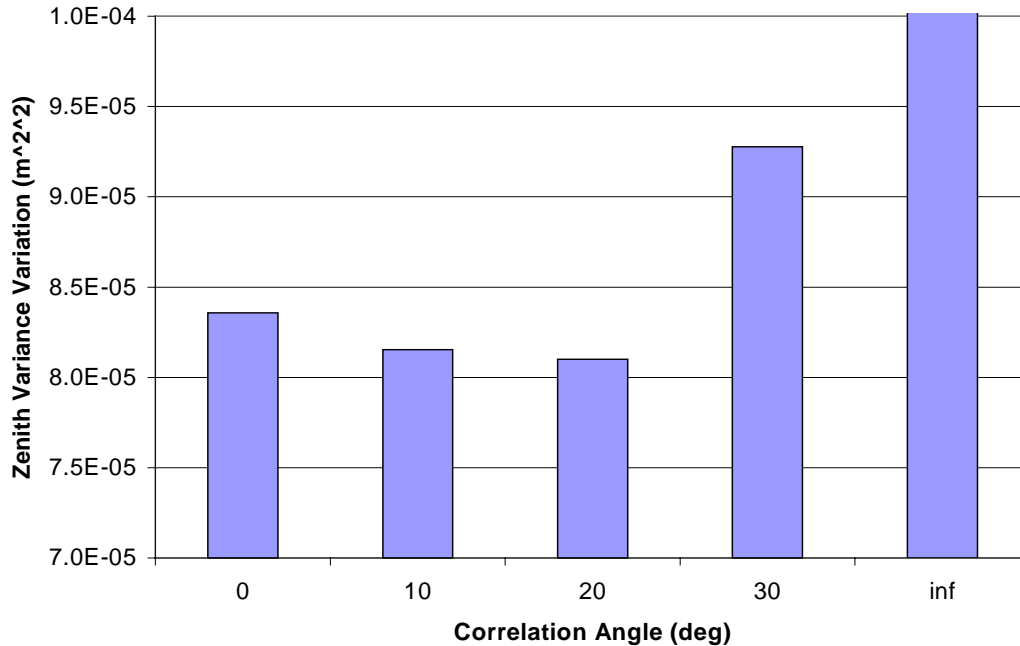


Figure 7. Mapped Zenith Variance Variation versus Assumed Correlation Angle

The final step in creating the tropospheric covariance model is to determine the accuracy of the tropospheric model and the correlation distance. To do this, all the binned elevation variances were mapped to zenith using a correlation angle value of 20°. The resulting zenith variances were averaged for each baseline and then plotted against receiver separation as in Figure (7), which illustrates the dependence of the double differenced variances with distance. To take into account the effect of multipath, a multipath variance parameter, σ_m^2 , was introduced which was assumed equal for all stations. A least squares fit of the tropospheric variance model plus multipath to the data produced a multipath standard deviation of 5mm, a tropospheric model accuracy of 2cm and a correlation distance of 350 kilometres. The corresponding curve is shown along with the data in Figure (7). The tropospheric model accuracy is approximately 50% better than that predicted by Collins and Langley, 1999, but the multipath variance is close to values stated by Radovanovic et al, 2000. Further research is required to determine if the correlation distance makes physical sense.

5.0 RIGOROUS ADJUSTMENT OF NETWORK DATA FOR KINEMATIC POSITIONING

Once the tropospheric model accuracy, angular correlation parameter, distance correlation length and multipath variance have been experimentally determined for a particular reference network, equation (13) can be used to create the double difference variance-covariance matrix for any combination of baselines. For example, if one wishes to position a mobile platform and (n) multiple stations are available, (n) unique baselines can be created which include the mobile platform. Using the variance model developed, the variance of double differences for each baseline can be predicted *as well as* the covariance between different baselines. The (n) baselines can then be processed together

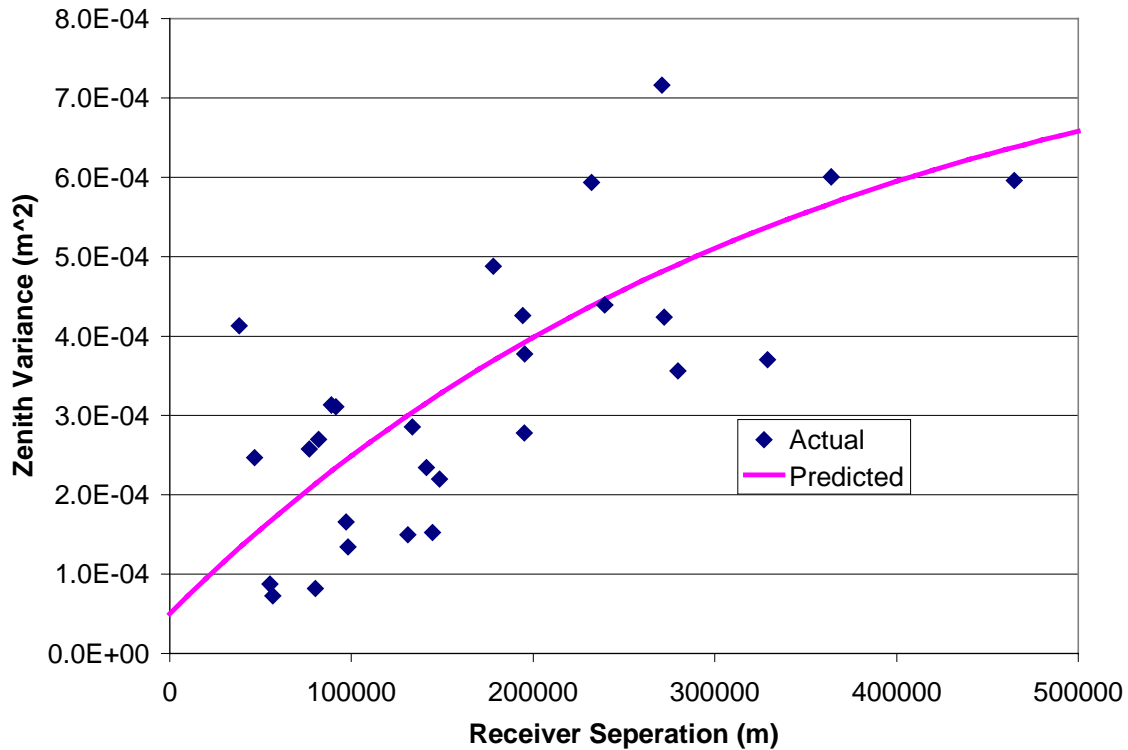


Figure 7. Actual and Predicted Zenith Variances (including Troposphere and Multipath)

in an epoch-by-epoch network adjustment overconstrained by fixing all the coordinates of the reference receivers. Overconstraining is preferred to inner-constraining or minimally constraining since the errors in the observations are assumed to be significantly greater than the errors in the reference coordinates.

As an example, station CHIL in the network analysed ($h_{el} = 1567.51$ m), was assumed to have unknown coordinates, thus simulating an airborne platform at heights typical for medium-scale aerial mapping. The data from CHIL was then processed with data at the other stations to determine its position over a two hour period. Three methods were used. Firstly, six independent baselines were processed and combined using a weighted mean scheme, where the weights were the estimated accuracies at each epoch. Secondly, all six baselines were combined into a network adjustment, but only mathematical correlations were assumed. Finally, the six baselines were simultaneously adjusted using the variance model developed. Figures (8) though (10) show the position estimates for each method. At any given epoch, the differences in the heights estimated by each method can reach 10 centimetres. Also, note that the station is actually static over the two hour period, so that any deviations from the mean position are actually errors. In particular, the height bias in the network adjustment with mathematical correlations only is striking. This is mainly due to incorrectly assuming that the zenith tropospheric errors between baselines are uncorrelated, and thus the double-differences independent between baselines.

Table 1 shows the RMS variation of the position estimates for the three processing methods along with the average estimated accuracy for each method over the two hours.

The rigorous adjustment method is the only one in which the RMS of the position estimates is lower than the average estimated accuracy. As well, the rigorous method has the lowest position variation of the three methods tested. This is significant in that it implies that not only does the rigorous method provide the most consistent results, it also provides the most robust statistics, which are important if the positioning accuracies are required, such as in photogrammetric block adjustment. In fact, if the a posteriori variance factors are calculated at each epoch when using the robust method, its average value over the two hour segment studied is 0.7, implying that the accuracy estimates are only slightly optimistic and validating the variance model.

Table 1. Comparison of Position RMS Values and Average Estimated Accuracies (values in centimetres)

Coordinate	Independent Baselines		Mathematical Correlations		Rigorous Adjustment	
	RMS	<i>Est. Acc. (1σ)</i>	RMS	<i>Est. Acc. (1σ)</i>	RMS	<i>Est. Acc. (1σ)</i>
N	1.4	<i>0.7</i>	1.4	<i>1.6</i>	1.2	<i>1.3</i>
E	1.0	<i>0.4</i>	1.5	<i>1.2</i>	0.8	<i>0.9</i>
H	3.5	<i>1.4</i>	7.0	<i>4.0</i>	3.0	<i>3.1</i>

6.0 CONCLUSIONS AND FUTURE WORK

When data is available from multiple receivers, it should be processed taking into account the correlations of the error sources affecting the carrier phases measured. If the correlations are not taken into account, then each sample of data is treated as if it was independent from other samples recorded at that epoch. This leads immediately to over-optimistic estimates and non-optimal estimation. Rather, it is important to use all data available together, and this includes variances and covariances.

To include variance and covariance data into adjustment of GPS data, a method of modeling the residual tropospheric variances has been presented which uses data collected from a reference network. Not only is correlation between stations significant, but also the correlation between satellites observed at a single station. Fortunately, both effects can be determined from collected data.

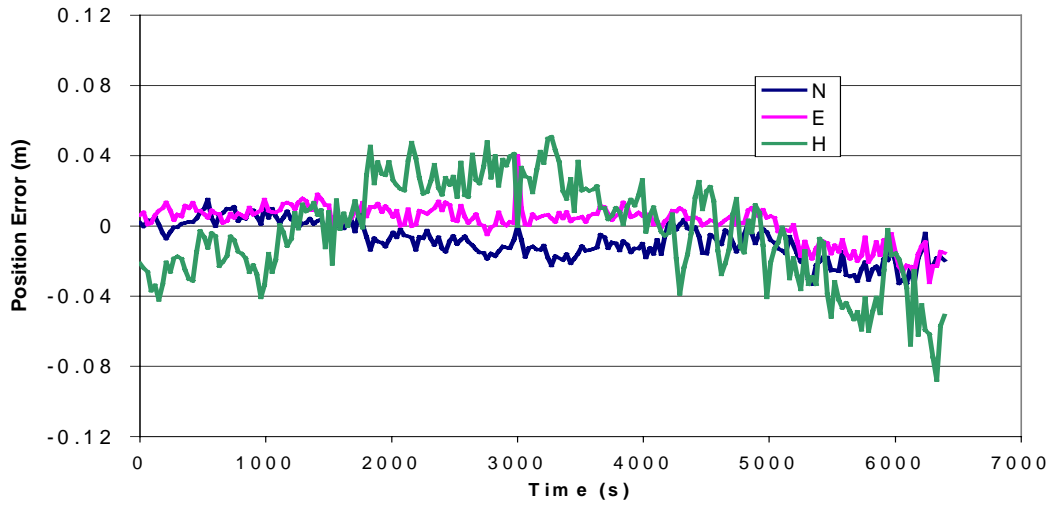


Figure 8. Position Error for Independent Baselines Method

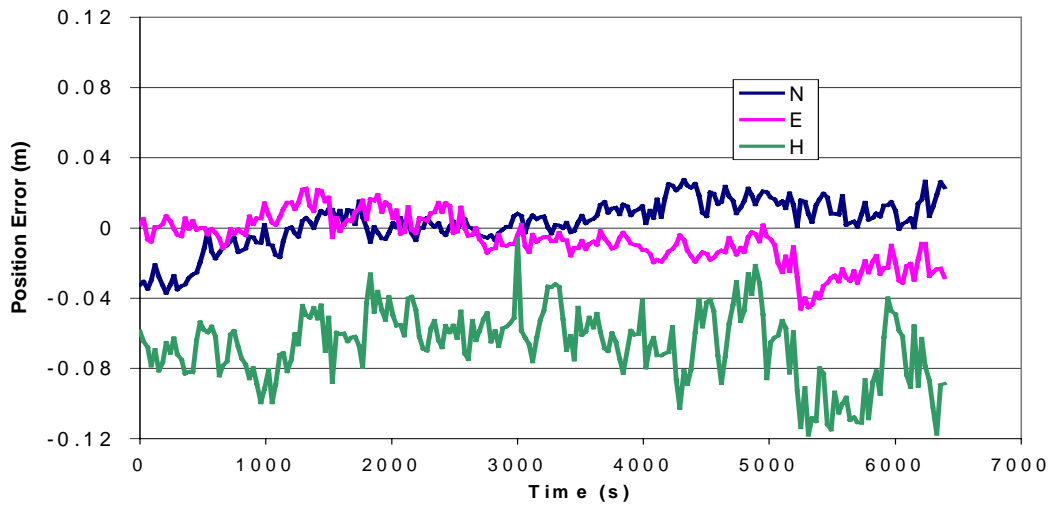


Figure 9. Position Error for Mathematical Correlation Modeling Method

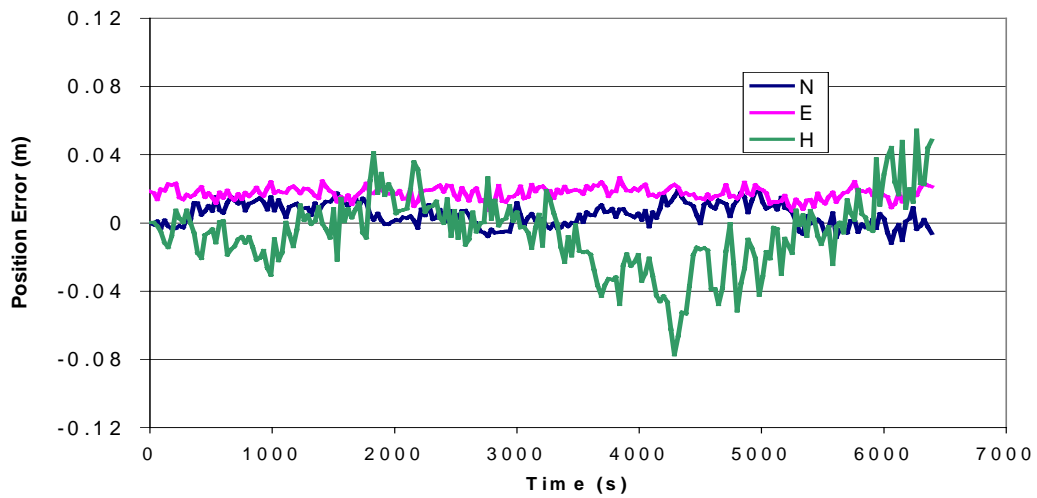


Figure 10. Position Error for Rigorous Variance Modeling Method

Once the variance model has been created, it can be used in a network adjustment of GPS measurements for positioning of mobile platforms. By including this model and simultaneously processing all data together, it was shown that improved positioning accuracies are achievable, resulting in 2 centimetre accuracies (1σ) in height from epoch-to-epoch by incorporating baselines ranging in length from 20 to 240 kilometres. Furthermore, the estimated positioning accuracies closely agreed with the position variations encountered.

Further work will focus on verifying achievable positioning accuracies under actual kinematic conditions. As well, it is important to study how the parameters for the tropospheric variance model change over time, or under various weather conditions. As well, improved methods of inverting the fully populated double difference variance-covariance are necessary, as it is a serious impediment to implementing the system in real time.

7.0 ACKNOWLEDGEMENTS

The authors would like to acknowledge the support of Challenger Surveys and Services, Ltd. in funding this research project.

8.0 REFERENCES

Collins, J.P. (1999). Assessment and Development of a Tropospheric Delay Model for Aircraft Users of the Global Positioning System. Technical Report No. 203. The University of New Brunswick.

Collins, J.P., R.B. Langley (1999). Nominal and Extreme Error Performance of the UNB3 Tropospheric Delay Model. Technical Report No. 204. The University of New Brunswick.

Hofmann-Wellenhof, B., H. Lichtenegger, J. Collins (1997). GPS : Theory and Practice. Springer-Verlag : New York.

Radovanovic, R., N. El-Sheimy, W.F. Teskey (2000). Development of a GPS-based Deformation Monitoring System : Vol III – Multipath and Noise. Technical Report. The University of Calgary.

Raquet, J. (1998) Development of a Method for Kinematic GPS Carrier-Phase Ambiguity Resolution Using Multiple Reference Receivers. Ph.D. Dissertation. The University of Calgary.